An X-band four-way combined GaN solid-state power amplifier*

Chen Chi(陈炽)†, Hao Yue(郝跃), Feng Hui(冯辉), Gu Wenping(谷文萍), Li Zhiming(李志明), Hu Shigang(胡仕刚), and Ma Teng(马腾)

(National Key Laboratory of Wide Band-Gap Semiconductor Technology, School of Microelectronics, Xidian University, Xi'an 710071, China)

Abstract: An X-band four-way combined GaN solid-state power amplifier module is fabricated based on a self-developed AlGaN/GaN HEMT with 2.5-mm gate width technology on SiC substrate. The module consists of an AlGaN/GaN HEMT, Wilkinson power hybrids, a DC-bias circuit and microstrip matching circuits. For the stability of the amplifier module, special RC networks at the input and output, a resistor between the DC power supply and a transistor gate at the input and $3\lambda/4$ Wilkinson power hybrids are used for the cancellation of low frequency self-oscillation and crosstalk of each amplifier. Under $V_{ds} = 27$ V, $V_{gs} = -4.0$ V, CW operating conditions at 8 GHz, the amplifier module exhibits a line gain of 5 dB with a power added efficiency of 17.9%, and an output power of 42.93 dBm; the power gain compression is 2 dB. For a four-way combined solid-state amplifier, the power combining efficiency is 67.5%. It is concluded that the reduction in combining efficiency results from the non-identical GaN HMET, the loss of the hybrid coupler and the circuit fabricating errors of each one-way amplifier.

Key words: AlGaN/ GaN HEMT; solid-state power amplifiers; Wilkinson hybrid coupler
DOI: 10.1088/1674-4926/31/1/015003 **EEACC:** 1350F; 1350H

1. Introduction

In radar and broadcast communication applications, T/R components are key elements. The performance of the T/R components will have an effect on the radar system. Inside these T/R components, the high-power amplifier is one of the very important microwave modules used in the final stages of radar and radio transmitters. Now, at high frequencies, high power amplifiers are based on GaAs PHEMT, MESFET and HBT transistors. However, due to the thermal and electrical limitations of GaAs transistors, the typical output power is low. To meet future requirements, higher output power levels, increased power-added efficiency values, and higher operating voltages are advantages for performance improvement. For these applications, AlGaN/GaN high electron mobility transistors (AlGaN/GaN HEMT) have been the subject of rapidly growing interest for high power applications. The key feature is that the GaN HEMTs have a high breakdown voltage, high carrier density, high saturation velocity and excellent thermal conductivity of the SiC substrate[1, 2]. In recent years, there have been several reports on the power performance of AlGaN/GaN HEMTs as discrete devices with very high output power densities[3, 4].

With the development of material growth and device fabrication technology, GaN-based amplifiers have received growing interest from the research community. AlGaN/GaN HEMT MMICs have been reported widely[5−8]. Recently, Piotrowicz[9] implemented a state-of-the-art GaN MMIC amplifier, whose size is 18 mm^2, and its output power reached 58 W. This result is the highest level in GaN-based power MMIC amplifiers.

Compared to MMIC amplifiers, the solid-state power amplifier (SSPA) can support higher power, higher reliability, and a longer run time. But there are few reports on the GaN solid-state amplifier in the development of GaN-based circuits[10]. In this paper, with microstrip matching technology, load pull measurement and the cut-try method, based on the self-developed AlGaN/GaN HEMT with 2.5-mm gate width technology on SiC substrate[11], we design and fabricate a four-way combined solid-state amplifier. To avoid SSPA instability, we use a $3\lambda/4$ separated branch transformer, RC stable networks and resistors between the DC power source and transistor gate. Under V_{ds} = 27 V and V_{gs} = −4.0 V, CW operating conditions at 8 GHz, the developed four-way combined solid-state amplifier with two 2.5-mm gate width AlGaN/GaN HEMTs demonstrated an output power of 42.93 dBm with a power added efficiency of 17.9% and a power combining efficiency of 67.5%. Finally, the reasons for the reduction in power combining efficiency are analyzed and illustrated.

2. Device technology

The sample was grown by the low-pressure MOCVD system on 4H-SiC substrate. Hydrogen was used as the carrier gas. Triethylgallium (TEGa), trimethylaluminum (TMAl) and ammonia (NH_3) were used as precursors. Prior to epitaxial growth, the 4H-SiC substrate was annealed at 1050 °C for 10 min in order to remove surface contamination. A 100-nm-thick high-temperature (HT) AlN nucleation layer was deposited, at 1100 °C. Then, the susceptor temperature was decreased to 1020 °C and a 2-μm-thick GaN layer was grown, followed by a 24-nm-thick undoped AlGaN barrier layer. The reactor pressure was kept at 40 Torr during growth. The Al component of the AlGaN layer was 30%. From Hall measurements, a room

* Project supported by the National Natural Science Foundation of China (Nos. 60736033, 60676048).
† Corresponding author. Email: ccachi@163.com
Received 6 July 2009, revised manuscript received 7 September 2009

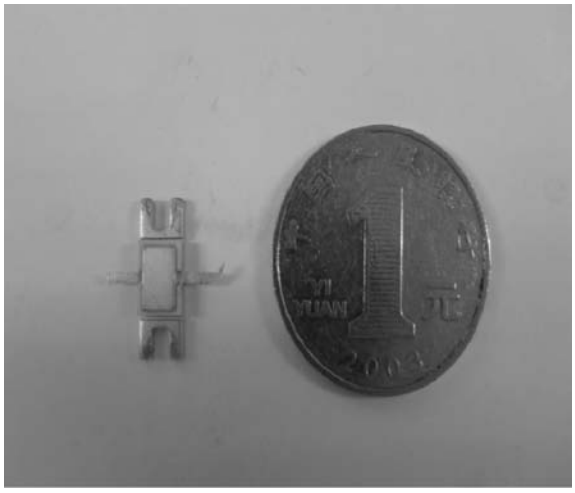

Fig. 1. External view of the GaN power HEMT.

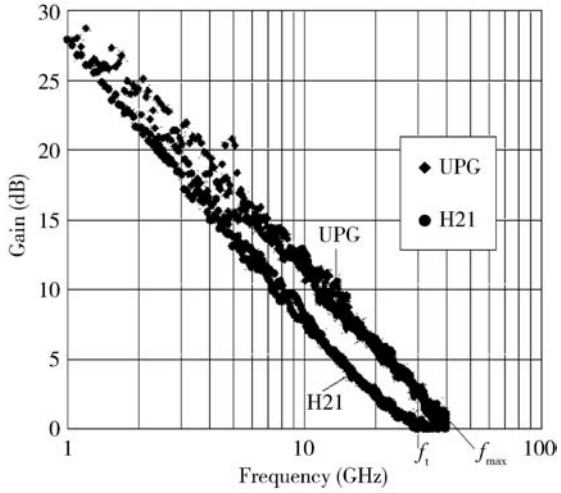

Fig. 2. Small performances of the GaN HEMT.

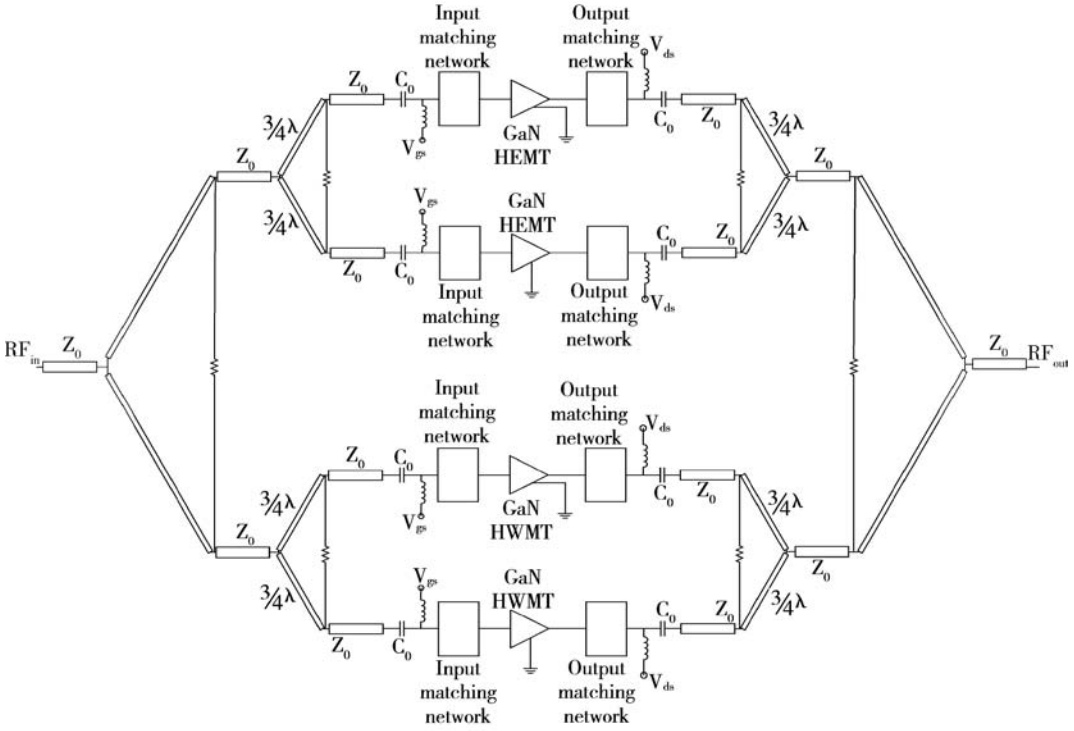

Fig. 3. Schematic diagram of the GaN-based four-way combined amplifier.

temperature mobility of 1570 $cm^2/(V \cdot s)$, a sheet carrier concentration of 1.29×10^{13} cm^{-2} and a sheet resistance of 308 $\Omega/\square$ have been obtained respectively. The device process follows standard HEMT processing technology. Device isolation was accomplished by Cl_2-based dry etching with an etching depth of about 150 nm; Ti/Al/Ni/Au (20 nm/120 nm/55 nm/45 nm) ohmic contact deposition was formed by electron-beam evaporation and annealing at 850 °C for 30 s, while Ni/Au (20 nm/200 nm) was utilized as a Schottky gate. After all these device processes, the SiN passivation layer was deposited by employing PECVD.

The device with a gate length of 0.4 μm and a gate width of 20 × 125 μm demonstrated an average saturation current 2 A/mm at a gate voltage of 1 V. The pinch-off voltage was −4.7 V. The packaged GaN high power transistor is shown in Fig. 1. The small signal performances of the GaN HEMT were measured by an Agilent E8364B network analyzer. As shown in Fig. 2, the current gain cut-off frequency f_t is 30 GHz and maximum oscillation frequency f_{max} is 39 GHz.

3. Solid-state amplifier design

3.1. Four-way combined GaN-based SSPA circuit design

Figure 3 shows a schematic diagram of the four-way Wilkinson hybrid combined solid-state power amplifier. The four-way combined SSPA was fabricated on the substrate by the microwave materials division of the Rogers Corporation. The size of the cavity can be calculated to prevent cavity reso-

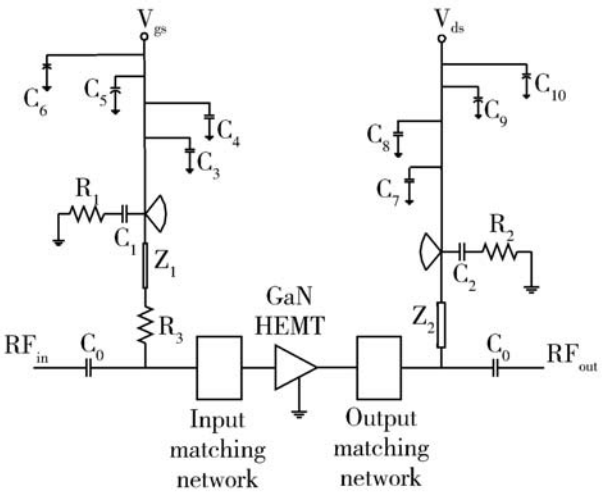

Fig. 4. The one-way amplifier circuit.

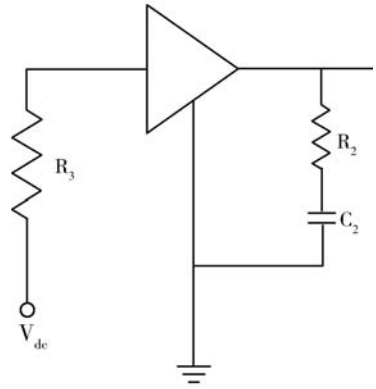

Fig. 5. Stability circuit of the one-way amplifier.

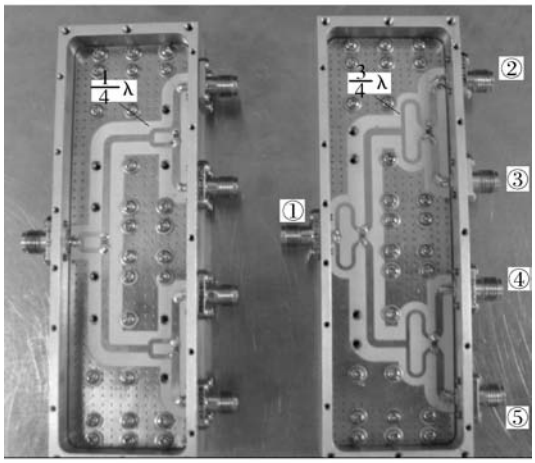

Fig. 6. Internal view of a λ/4 Wilkinson hybrid coupler and a 3λ/4 Wilkinson hybrid coupler.

nance[12].

The amplifier module consists of Wilkinson couplers, an input matching circuit, an output matching circuit and a DC-biased circuit. The four-way GaN-based amplifiers are connected in parallel with the two-stage Wilkinson hybrid couplers, which operate as a power divider at the input and a power combiner at the output, respectively.

3.2. Bias circuit, matching circuit and stability circuit

For each one-way amplifier, a bipolar DC power source is used as shown in Fig. 4. The characteristic impedances of Z_1 and Z_2 are 128 Ω and 109 Ω, respectively. The lengths of both are 1/4 microstrip wavelength. The radial stubs are open to the odd harmonious wave and short to the even harmonious wave, which is useful to prevent the leakage of energy from the bias network and promote the linearity and output power of the amplifier. At the same time, the radial stubs can improve the microwave performances of the power device in output power and gain[13]. C_3, C_4, C_7, C_8 are decoupling capacitances filtering the noise from the DC power, and C_5, C_6, C_9, C_{10} can prevent the interference of low frequency signal with the DC power. The C_0 is RF single coupling capacitance, which can isolate the DC current.

The external matching circuit is mainly based on the auto-load pull measurement and cut-try method with microstrip foil. On the basis of the auto-load pull measurement of the packaged large gate periphery transistor, the matching networks are designed and adjusted. The output power and power-added efficiency are monitored by changing the length and width of the microstrip stub at special positions at the input and output ports. The maximum output power and the optimum power-added efficiency can then be obtained.

There are four approaches to improve the stability of the amplifier[14]. In Fig. 5, one of the stability networks is illustrated. The resistor R_3 between DC power and the transistor gate is used to improve the stability and prevent self-oscillation of the amplifier. The resistor R_2 and C_2 can also improve the stability, and the capacitor C_2 can avoid the DC power consumption of resistor R_2.

3.3. Wilkinson power hybrid coupler

The two-stage Wilkinson hybrid has the advantages of simple construction and high port-to-port isolation[15]. In our design, 3λ/4 for the branch coupler rather than the traditional λ/4 is used as shown in Fig. 6, because in the X-band, the electrical length of 90° of the standard symmetrical Wilkinson output branches must be placed very close to each other to connect the surface mounted resistor. This will give rise to strong mutual coupling between the output lines[16],which can cause serious self-oscillation serious. However, a Wilkinson power divider and combiner with semi-circle 3λ/4 arms can separate the branches widely and eliminate self-oscillation effectively.

The ADS co-simulated results and measured results of the 3λ/4 microstrip branch are plotted in Fig. 7. The simulated and measured insertion losses are plotted in Fig. 7(a). The measured insertion losses are between 0.5 dB and 1.8 dB in the band. In Fig. 7(b), the return losses are described. The measured return loss in the input port is 10 dB and the return losses in the output ports are between 10 dB and 40 dB in the band. The isolation results are shown in Fig. 7(c). The measured isolations between the closer ports (port ② and port ③, port ④ and port ⑤, as shown in Fig. 6) are between 14 dB and 16 dB across band, and the isolations between the further ports (port ② and port ④, port ② and port ⑤, port ③ and port ④, port ③

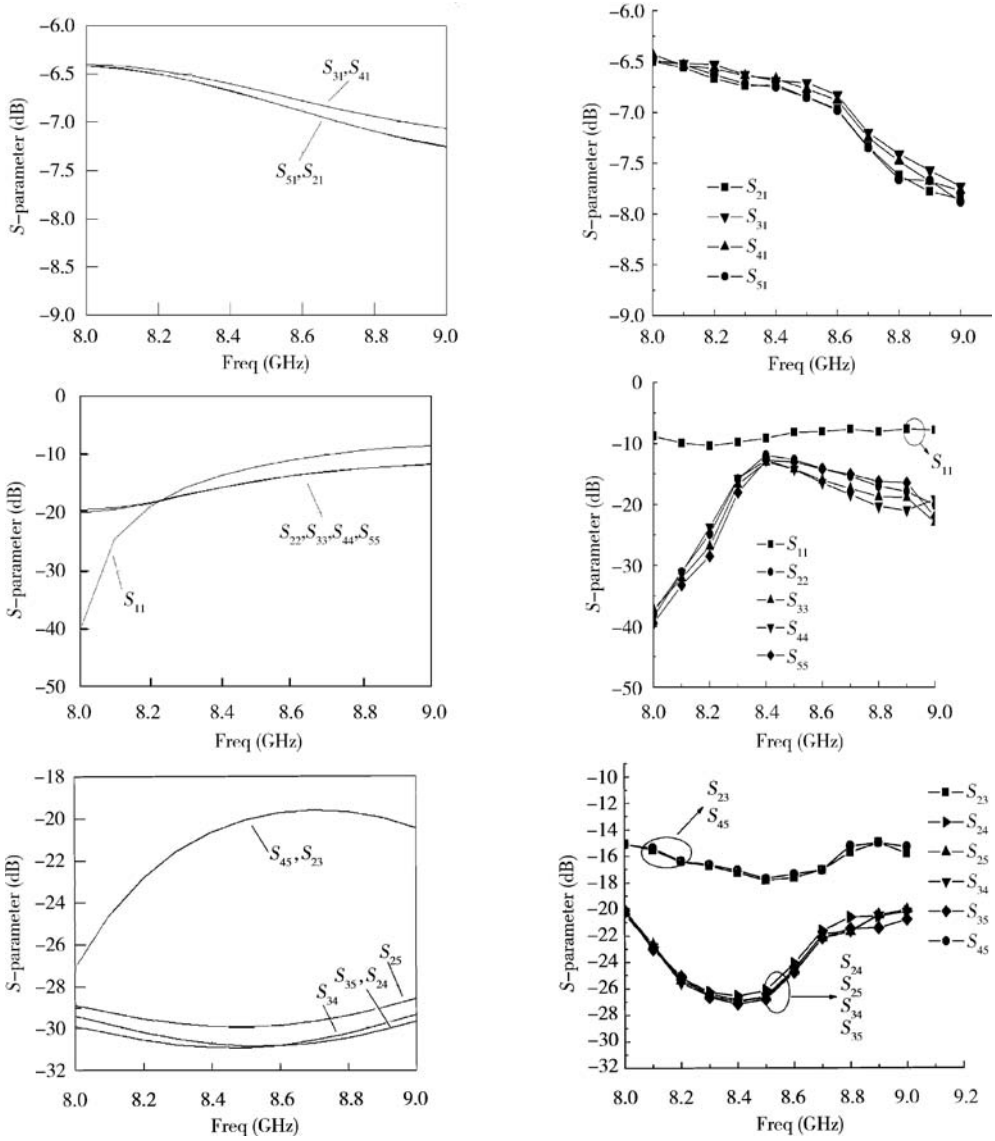

Fig. 7. Simulated and measured S parameters of the $3\lambda/4$ Wilkinson hybrid.

and port ⑤) are between 20 dB and 30 dB.

Compared to the simulated results, the tendency of the measured results is nearly the same between 8 GHz and 9 GHz, but the simulated results are better than the measured results. The difference is caused by three reasons. Firstly, the large size of the $3\lambda/4$ hybrid coupler can result in redundant conductor losses. The other two reasons are substrate dielectric losses and microstrip radiation losses[17].

4. Large-signal measurements of the four-way combined GaN HEMT SSPA

The large signal measurement system includes an HP8350B sweep oscillator, an HP437B power meter, an HP8593A spectrum analyzer and another microwave measurement assembly. The driver amplifier can deliver an output power of 40 dBm in the X band.

In Fig. 8, large single measurements of the four-way combined amplifier were performed with a drain bias voltage of 24 V and a gate bias voltage of – 4.0 V. The largest linear gain

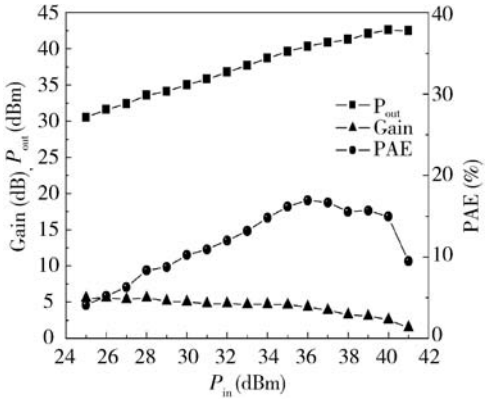

Fig. 8. Measured power performances of the four-way combined GaN HEMT SSPA at 8 GHz with $V_{ds} = 24$ V and $V_{gs} = -4.0$ V, $P_{outmax} =$ 42.58 dBm.

was 5.5 dB. The output power at the 1 dB gain compression point was 39.6 dBm. The maximum output power was 42.58

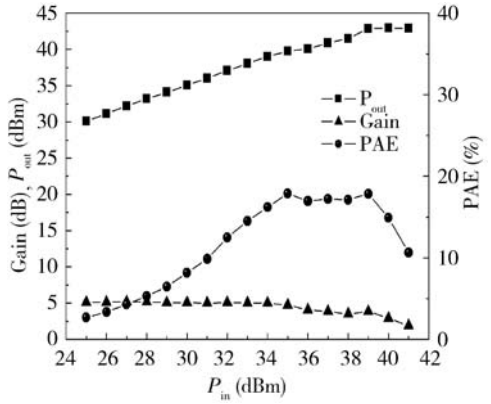

Fig. 9. Measured power performances of the four-way combined GaN HEMT SSPA at 8 GHz with V_{ds} = 27 V and V_{gs} = −4.0 V, P_{outmax} = 42.93 dBm.

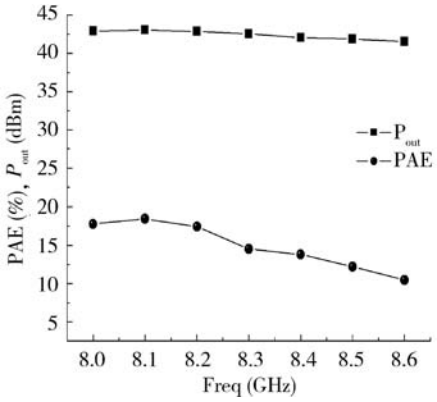

Fig. 10. Measured output power and PAE against frequency of the four-way combined GaN HEMT SSPA at P_{in} = 40 dBm with V_{ds} = 27 V and V_{gs} = −4.0 V.

dBm and the corresponding gain compression was 3 dB. In Fig. 9, large single measurements were performed with a drain bias voltage of 27 V and a gate bias voltage of −4.0 V. The largest linear gain was 5 dB. The output power at the 1 dB gain compression point was 40.07 dBm. When the input power was 40 dBm, a maximum output power of 42.93 dBm was achieved and the corresponding gain compression was 2 dB. A maximum PAE of 17.9% was obtained at an input power of P_{in} = 35 dBm.

The dependence of output power and PAE on frequency is shown in Fig. 10. The measurement conditions were V_{ds} = 27 V, V_{gs} = −4.0 V. As shown in Fig. 10, the variation of output power between 8 GHz and 8.5 GHz is less than 1.5 dB, and with increasing frequency, both the maximum saturated output power and the PAE decreased. Figures 11 and 12 show internal and external views of the four-way combined GaN HEMT solid-state amplifier.

5. Results and discussion

5.1. Calculation of power combining efficiency

The test fixture for the one-way amplifier is shown in Fig. 13. In Fig. 14, the power performances for every amplifying unit are displayed. Large signal measurements

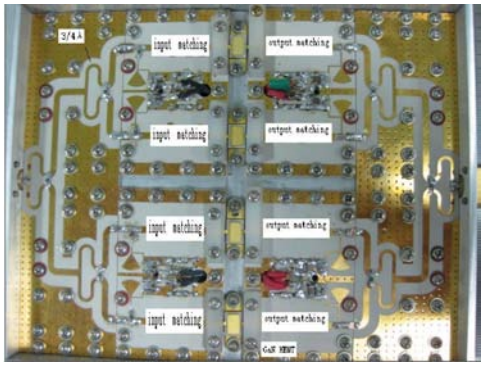

Fig. 11. Internal view of the four-way combined GaN HEMT SSPA.

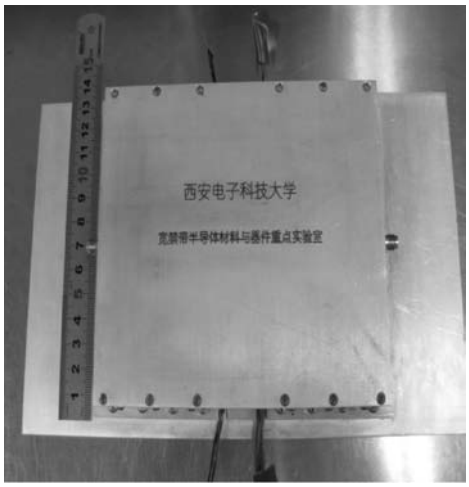

Fig. 12. External view of the four-way combined GaN HEMT SSPA.

of the single transistor amplifier were performed at V_{ds} = 27 V and V_{gs} = −4.0 V. In Fig. 14, the amplitude of every GaN HEMT is unbalanced. When the input power is 35 dBm, the maximum output powers are 38.54, 39, 38.5 and 38.42 dBm and the corresponding linear gains are 6, 6, 5.9 and 5.6 dB, respectively. According to the power combining efficiency formula, the power combining efficiency in our experiments is:

$$\eta_c = \frac{p_{out}}{4p_{single}} = \frac{p_{out}}{P_1 + P_2 + P_3 + P_4}$$

$$= \frac{19.63\text{W}}{7.14\text{W} + 7.94\text{W} + 7.07\text{W} + 6.95\text{W}} = 67.5\%. \quad (1)$$

5.2. Discussion of power combining efficiency error

The N-stage power combining network and two-stage power combining network we used are shown in Fig. 15. In practical systems, the insertion loss of the hybrid coupler can cause a reduction in total added power and combining efficiency, and can then impose an upper limit on the number of amplifiers which can be combined.

When only considering the loss of the hybrid coupler, the expected output power, linear gain and power combining efficiency are given by the formulas[18]:

$$P_{out} = 2^k L_h^{-K} P_0, \quad (2)$$

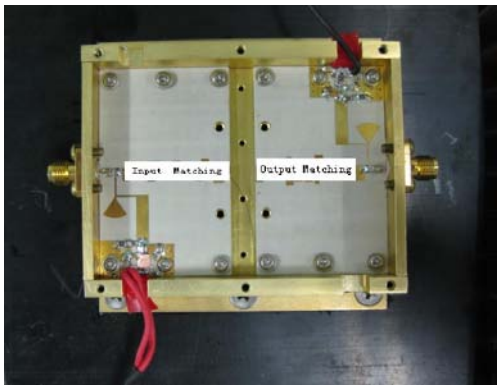

Fig. 13. Test fixture for the one-way amplifier.

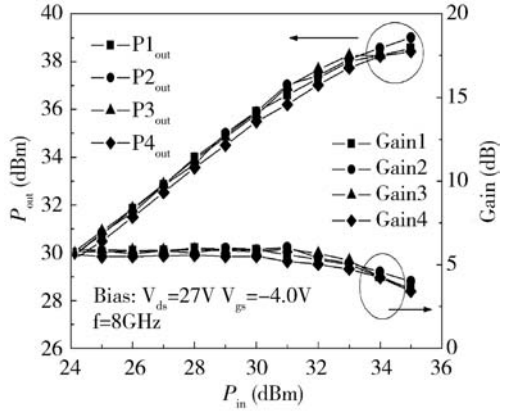

Fig. 14. Measured output power and gain for each one-way amplifier.

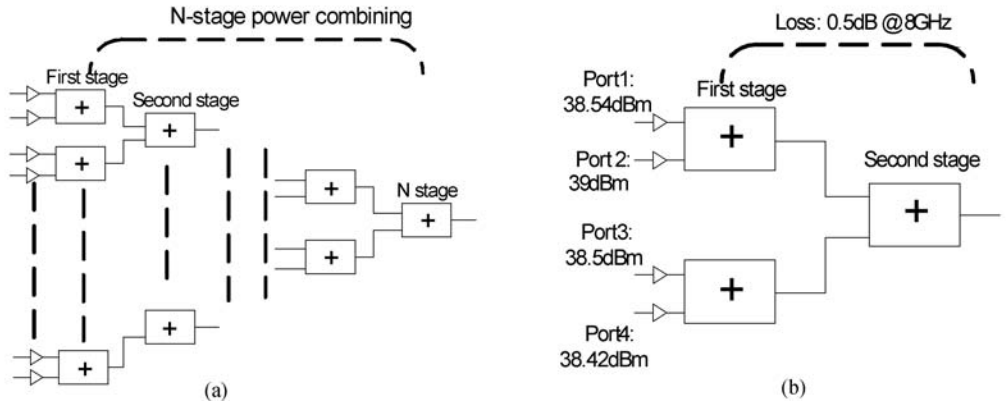

Fig. 15. Power combining schematic. (a) N-stage power combining network. (b) Two-stage power combining network in our experiment.

$$G_{\mathrm{t}} = L_{\mathrm{h}}^{-2} G_{\mathrm{i}}, \tag{3}$$

$$\eta_{\mathrm{c}} = \frac{P_{\mathrm{add}}}{NP_0} = L_{\mathrm{h}}^{-K}, \tag{4}$$

where k is the stage of the hybrid combiner, L_{h} the insertion loss of the hybrid coupler, P_0 the individual amplifier output power and G_{i} the individual amplifier gain. Assuming that the individual devices are similar, these formulas are applicable.

In Fig. 15(b), the stage of the hybrid coupler is two, and with the results of output power and gain, we can get an expected combining efficiency of 79.7%, a total output power of 22.5 W and a gain of 5.01 dB. Compared to our measured power performances, there is a decrease in the measured output powers and power combining efficiencies, but the gains are the same. The reason for this is that amplitude imbalance and phase error of individual amplifiers can also cause a decrease in output power and power combining efficiency excluding the gain.

For the one-stage power combining network, the output power and power combining efficiency can be expressed by the formulas[19]:

$$P_0 = \frac{1 + 10^{D/10} + 2\cos\theta \times 10^{D/20}}{2} \times P_1, \tag{5}$$

$$\eta_{\mathrm{c}} = \frac{P_0}{P_{\mathrm{in}}} = \frac{1 + 10^{D/10} + 2\cos\theta \times 10^{D/20}}{2\left(1 + 10^{D/10}\right)}, \tag{6}$$

where θ is the phase difference between the two input powers and D is the amplitude imbalance between two input powers P_1 and P_2, which can be expressed as:

$$D(\mathrm{dB}) = 10\lg\frac{p_2}{p_1} = P_2(\mathrm{dBm}) - P_1(\mathrm{dBm}). \tag{7}$$

Basically, phase error is much more critical than amplitude imbalance in an amplifier for good combining efficiency. A higher than 90% combining efficiency can be obtained for amplitude imbalances from –3 dB to +3 dB, when the phase error is kept within 30°[20]. In our experiments, the amplitude differences between the two ports are 0.5 dB and 0.1 dB, respectively. So the phase deviation and amplitude differences cause the combining efficiency and output power to decrease.

The amplitude imbalance and phase deviation are caused by different characteristics of GaN HEMTs (DC-IV performances, S parameters and large signal performances of device), different microstrip matching networks and fabrication errors for every one-way amplifier. Therefore, to get a high combining efficiency and output power, amplitude balance and an appropriate phase relationship for the different transistors, a low loss hybrid coupler and accurate microstrip fabricating technology are necessary.

6. Conclusion

A four-way combined GaN HEMT solid-state amplifier module has been developed. Because of the potential instability

of the amplifier, the RC stable network and the resistor between the DC power source and the transistor gate were designed to make the amplifier stable. In the design of the Wilkinson divider/combiner, in order to ensure amplifier module stability, $3\lambda/4$ transmission-lines were used to decrease the coupling of the microstrip. Under V_{ds} = 27 V, V_{gs} = –4.0 V, CW operating conditions at 8 GHz, the developed four-way combined solid-state amplifier delivered an output power of 42.93 dBm with power added efficiency of 17.9%, and a power combining efficiency of 67.5% at 8 GHz was obtained. Compared to the calculated value, the reasons for the reduction in power and power combining efficiency are illustrated. To get a high power combining efficiency and output power for the amplifier module, identical GaN HEMT and low loss hybrid couplers must be designed and selected.

References

[1] Trew R J, Bilbro G L, Kuang W, et al. Microwave AlGaN GaN HFETs. IEEE Microw Mag, 2005, 6(1): 56

[2] Mishra U K, Parikh P, Wu Y F. AlGaN/GaN HEMTs–an overview of device operation and applications. Proc IEEE, 2002, 90(6): 1022

[3] Wu Y F, Saxler A, Moore M, et al. 30-W/mm GaN HEMTs by field plate optimization. IEEE Electron Device Lett, 2004, 25(3): 117

[4] Takagi K, Masuda K, Kashiwabara Y, et al. X-band AlGaN GaN HEMT with over 80 W output power. Compound Semiconductor Integrated Circuit Symposium, 2006: 265

[5] Schuh P, Leberer R, Sledzik H, et al. 20 W GaN HPAs for next generation X-band T R-modules. Microwave Symposium Digest, 2006: 726

[6] Wurfl J, Behtash R, Lossy R, et al. Advances in GaN-based discrete power devices for L- and X-band applications. Microwave Conference, 2006: 1716

[7] Moon J S, Wong D, Antcliffe M, et al. High PAE 1 mm AlGaN/GaN HEMTs for 20 W and 43% PAE X-band MMIC amplifiers. Electron Devices Meeting, 2006: 1

[8] Meliani C, Behtash R, Wurfl J, et al. A Broadband GaN-MMIC power amplifier for L to X bands. Microwave Integrated Circuit Conference, 2007: 147

[9] Piotrowicz S, Morvan E, Aubry R, et al. State of the art 58 W, 38% PAE X-band AlGaN/GaN HEMTs microstrip MMIC amplifiers. Compound Semiconductor Integrated Circuits Symposium, 2007: 1

[10] Kanto K, Satomi A, Asahi Y, et al. An X-band 250 W solid-state power amplifier using GaN power HEMTs. Radio and Wireless Symposium, 2008: 77

[11] Wang Chong, Hao Yue, Zhang Jincheng. Development and characteristics of AlGaN/GaN HEMT. Journal of Xidian University, 2005, 32(2): 234 (in Chinese)

[12] Writing team of microstrip circuits from Tsinghua University. Microstrip circuits. Beijing: Post and Telecom Press, 1976

[13] Luo Weijun, Chen Xiaojuan, Liang Xiaoxin, et al. A radial stub test circuit for microwave power devices. Chinese Journal of Semiconductors, 2006, 27(9): 1557

[14] Gonzalez G. Microwave transistor amplifiers analysis and design. 2nd ed. New Jersey: Prentice Hall, 1997

[15] Wilkinson E J. An N-way hybrid power divider. IEEE Trans Microw Theory Tech, 1960, 1: 116

[16] Horst S, Bairavasubramanian R, Tentzeris M M, et al. Modified Wilkinson power dividers for millimeter-wave integrated circuits. IEEE Trans Microw Theory Tech, 2007, 55(11): 2439

[17] Antsos D, Crist R, Sukamto L. A novel Wilkinson power divider with predictable performance at K and Ka-band. Microwave Symposium Digest, 1994, 5: 907

[18] Kuno H J, David L. Millimeter-wave IMPATT power amplifier/combiner. IEEE Trans Microw Theory Tech, 1976, 24(11): 758

[19] Joseph R, Gerald J. Output power and loss analysis of 2^n injection-locked oscillators combined through an ideal and symmetric hybrid combiner. IEEE Trans Microw Theory Tech, 1969, 17(1): 1

[20] Chang K, Sun C. Millimeter-wave power-combining techniques. IEEE Trans Microw Theory Tech, 1983, 31(2): 91